Journal of Electronic Research and Application, 2025, Volume 9, Issue 3
http://ojs.bbwpublisher.com/index.php/JERA
ISSN Online: 2208-3510
ISSN Print: 2208-3502

Research on Low-Speed Performance Optimization of BLDC without Position Sensors Based on EKF

Wei Liu, Yakun Wang*

School of Information and Control Engineering, Jilin Institute of Chemical Technology, Jilin 132022, Jilin, China

**Author to whom correspondence should be addressed.*

Abstract: To obtain real-time rotor information of the brushless DC motor, improve the low-speed performance and anti-interference ability of the motor, a sensorless vector control system model of the brushless DC motor was established. A motor control system based on the EKF algorithm was designed. By combining the EKF observer with the brushless DC motor, a simulation model of the EKF motor control system was built based on Simulink. The simulation results show that the motor control system with the EKF observer operates well. The motor's low-speed operation performance and rotor position detection are very fast, and the motor's anti-interference ability is significantly enhanced, effectively improving the dynamic performance of the control system [1].

Keywords: Brushless DC motor; EKF; Motor control

Online publication: 6 June, 2025

1. Introduction

Brushless DC motors (BLDCM) are increasingly being used in industrial robots, intelligent devices, and other fields due to their advantages, such as wide speed regulation range, high efficiency, simple structure, and long service life. To achieve precise control of BLDC, high-precision sensors are usually used directly to obtain the real-time position of the motor rotor, which makes the overall cost of the motor control system high. The sensors cannot perform at their full capacity in the face of interference from the external environment, resulting in significant fluctuations in control effect. As a result, sensorless detection technology is gradually becoming a trend in the development of brushless DC motor vector control systems. Currently, sensorless vector control technologies mainly include model reference adaptive control, sliding mode observer control, Kalman filter control, etc [2]. ETF is based on the mathematical model of the brushless DC motor, and through different iterative operations, it acquires the optimal estimate in two parts: the predicted estimate and the corrected estimate, to achieve the observation of the motor state. Compared with other control methods, the advantage of the extended Kalman filter is for complex nonlinear equations, while the state space equation of the brushless DC motor is nonlinear. EKF is applied to the speed control system of the brushless DC motor through the operation of linearizing nonlinear systems and discretizing continuous systems.

To further improve the low-speed performance of the motor and enhance the anti-interference ability of BLDC, this paper takes the brushless DC motor as the research object to study the EKF algorithm, derive the linear Kalman estimation for the extended Kalman (EKF) optimal estimation, and combine the EKF observer with the brushless DC motor. Based on the EKF algorithm, a sensorless motor vector control system simulation model was built. By comparing with the FOC vector control system with a position sensor, the speed tracking experiment and rotor position tracking experiment of BLDC running at low speed were completed to verify the good low-speed performance of the EKF algorithm combined with the real motor [3].

2. Mathematical model of a brushless DC motor

In this paper, the inner rotor type brushless DC motor is used as the research object. The stator windings of the motor are connected in a star pattern and conduct two by two. The equivalent circuit diagram of the brushless DC motor is shown in **Figure 1** below:

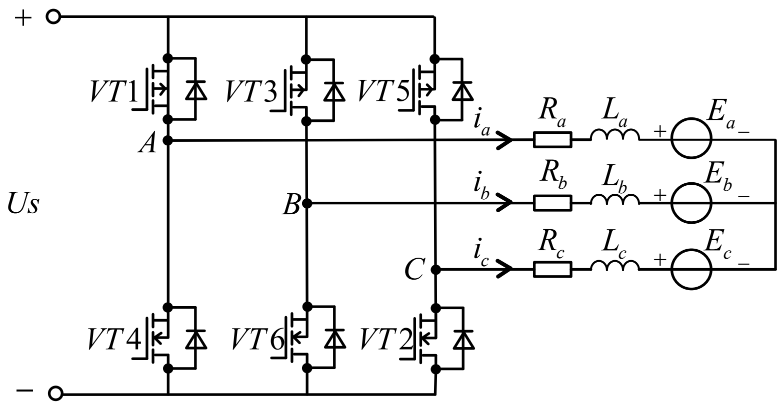

Figure 1. Equivalent circuit diagram of a brushless DC motor

From the equivalent circuit diagram combined with the simplified conditions, the voltage equations of the three-phase windings of the stator and the torque equations of the motor in the three-phase stationary coordinate system can be obtained as follows:

$$\begin{bmatrix} u_a \\ u_b \\ u_c \end{bmatrix} = \begin{bmatrix} R_a & 0 & 0 \\ 0 & R_b & 0 \\ 0 & 0 & R_c \end{bmatrix} \begin{bmatrix} i_a \\ i_b \\ i_c \end{bmatrix} + p \begin{bmatrix} \psi_a \\ \psi_b \\ \psi_c \end{bmatrix} \tag{1}$$

$$T_e = \frac{1}{2} p_n \frac{\partial}{\partial \theta_m} (i_{3s}^T \cdot \psi_{3s}) \tag{2}$$

Among them, $u_a u_b u_c$ are the three-phase terminal voltages of the stator windings; R_a,R_b,R_c are the resistances of each phase winding; i_a,i_b,i_c are the three-phase stator currents of each phase; p is the differential operator d/dt; ψ_a,ψ_b,ψ_c are the back electromotive forces (EMFs) generated by the permanent magnets of the rotor; T_e is the electromagnetic torque; p_n is the number of pole pairs of the brushless DC motor; θ_m is the mechanical angular displacement; i_{3s}^T represents the transpose of the three-phase current matrix; ψ_{3s} denotes the three-phase flux linkage matrix [4].

Based on the principle of keeping the magnetomotive force (MMF) unchanged, the three-phase stationary coordinate system is transformed into a two-phase stationary coordinate system through the *Clark* transformation.

$$\begin{cases} u_\alpha = Ri_\alpha + L_s \frac{di_\alpha}{dt} - \omega_e \psi_f \sin\theta \\ u_\beta = Ri_\beta + L_s \frac{di_\beta}{dt} - \omega_e \psi_f \cos\theta \end{cases} \tag{3}$$

For the sake of analysis, the mathematical model of the brushless DC motor in the natural coordinate system needs to be simplified. After the coordinate transformation simplification, the stator voltage equation and electromagnetic torque equation of the brushless DC motor in the synchronous rotating coordinate system are respectively:

$$\begin{cases} u_d = Ri_d + L_d \frac{di_d}{dt} - \omega_e L_q i_q \\ u_q = Ri_q + L_q \frac{di_q}{dt} - \omega_e (L_d i_d + \psi_f) \end{cases} \tag{4}$$

$$T_e = \frac{3}{2} P_n \left[\psi_f i_q + (L_d - L_q) i_d i_q \right] \tag{5}$$

In the equation, u_d and u_q represent the stator voltages on the *d*-axis and *q*-axis, respectively; represents the equivalent resistance of the armature winding; i_d and i_q are the stator current components on the *d*-axis and *q*-axis, respectively; L_d and L_q denote the stator inductances on the *d*-axis and *q*-axis, respectively; ω_e is the motor speed; ψ_f is the permanent magnet flux linkage, which can be treated as a constant when temperature effects are neglected.

3. EKF algorithm Implementation

3.1. Introduction to EKF algorithm theory

Kalman filtering, an extension of traditional filtering theory, is an optimized algorithm for predicting system states. It combines the dynamic model of the system with sensor data. By recursively, the state estimation is updated when the sensor measures, and the next state is predicted [5]. Suppose there is the following linear equation:

$$\begin{cases} x_k = Ax_{k-1} + Bu_k + w_k \\ Z_k = Hx_k + v_k \end{cases} \tag{6}$$

In the above equation, x_k is the discrete state variable at the time step *k*, x_{k-1} is the system state transition matrix from time step *k–1* to time *k*, Z_k is the observed variable, u_k is the system input vector, *A* is the state matrix, *B* is the control matrix, *H* is the measurement matrix, w_k is the system noise, v_k is the measurement noise.

$p(w) \sim N(0,Q)$ Where 0 represents the expectation and *Q* is the covariance matrix of the process noise; $p(V) \sim N(0,R)$0 represents expectation, *R* representing the covariance matrix of the measurement noise. The linear EKF observer implementation process is as follows:

(1) Prior state values:

$$\hat{x}_{\bar{k}} = A\hat{x}_{k-1} + Bu_{k-1} \tag{7}$$

Where $\hat{x}_{\bar{k}}$ is the priori estimate for the *k* order, $\hat{x}_{k-1}$ is the posterior estimate for the *k–1* order, u_{k-1} is the control matrix for the *k–1* order.

(2) Prior error covariance:

$$P_{\bar{k}} = AP_{k-1}A^T + Q \tag{8}$$

Where $P_{\bar{k}}$ is the prior estimate error covariance matrix of the *k* order, P_{k-1} is the error covariance matrix of the *k–1* order.

(3) Kalman gain

$$K_k = \frac{P_{\bar{k}} H^T}{(H P_{\bar{k}} H^T + R)} \tag{9}$$

(4) Correcting estimates:

$$\hat{x}_k = \hat{x}_{\bar{k}} + K_k (Z_k - H \hat{x}_{\bar{k}}) \tag{10}$$

(5) Update the covariance matrix for the next moment:

$$P_k = (I - K_k H) P_{\bar{k}} \tag{11}$$

Where P_k is the error covariance matrix of the k time, I is the identity matrix.

3.1.1. EKF prediction

Predict the optimal estimate of the moment based on the optimal estimate of the moment. *k–1k*

$$\hat{x}_{k|k-1} = \phi_{k|k-1} \hat{x}_{k-1|k-1} \tag{12}$$

Among them, $\hat{x}_{k|k-1}$ represents the a priori state estimate at the time step k predicted from the time step $k–1$, $\hat{x}_{k-1|k-1}$ is the estimated value at time $k–1$, and $\phi_{k|k-1}$ is the state transition matrix from time to time [6].

$$P_{k|k-1} = \phi_{k|k-1} P_{k-1|k-1} \phi_{k|k-1}{}^T + Q \tag{13}$$

Among them, the predicted mean square error is calculated, where Q is the systematic error of the predicted mean square error.

3.1.2. Update phase

$$k_{k|k-1} = P_{k|k-1} c^T (c P_{k|k-1} c^T + R)^{-1} \tag{14}$$

$$\hat{x}_{k|k} = \hat{x}_{k|k-1} + k_{k|k-1} (y_k - \hat{y}_{k|k-1}) \tag{15}$$

$$P_{k|k} = (I - k_{k|k-1} c) P_{k|k-1} \tag{16}$$

3.2. Extended Kalman filter optimal estimation

Extended Kalman filtering pushes EKF's best estimation in the linear domain to the nonlinear domain for complex nonlinear equations, which involves two steps [7]: linearization of nonlinear systems and discretization of continuous systems.

3.2.1. Linearization of nonlinear systems

Suppose there are the following linear system equations in the continuous field:

$$\dot{x} = f(x(t), u, t) + w(t) \tag{17}$$

Where, $\dot{x}$ represents the derivative of x, f is a nonlinear function, $w(t)$ is the system noise. The linear system space expression after linearization can be expressed as:

$$\begin{cases} \dot{x} = Ax + Bu + w(t) \\ y = cx \end{cases} \tag{18}$$

A is $\frac{\partial f(x(t),u,t)}{\partial x}|_{x(t)=\dot{x}(t)}$, B is the coefficient of the input matrix.

3.2.2. Discretization of continuous systems

The essence of discretization of continuous systems is to convert the equations in the continuous domain into differential equations that the microcontroller can handle by the definition of derivatives. The discretized equation can be expressed as:

$$\hat{x}_{k|k-1} = \hat{x}_{k-1|k-1} + (\phi_{k|k-1}\hat{x}_{k-1|k-1} + Bu)T_s \qquad (19)$$

In the formula, represents the input; indicates the sampling period [8].

4. EKF algorithm state observer combined with brushless DC motor

When the EKF algorithm state observer is combined with a brushless DC motor, stable output regulation and closed-loop control can be achieved in the motor speed control system [9]. The state space expression of EKF can be expressed as:

$$\begin{cases} \frac{d\hat{x}(t)}{dt} = A\hat{x}(t) + Bu(t) + K(y(t) - \hat{y}(t)) \\ \hat{y}(t) = c\hat{x}(t) \end{cases} \qquad (20)$$

When discretized, it can be expressed as:

$$\begin{cases} \hat{x}_k = A\hat{x}_{k-1} + Bu_k + K(y_k - \hat{y}_k) \\ y_k = c\hat{x}_{k|k-1} \end{cases} \qquad (21)$$

Combined with the *Clark* transformation dimensionality reduction of the motor equation, the system state variable is $x_k = (i_\alpha, i_\beta, \omega_e, \theta)^T$, the output variable is $u_k = (u_\alpha, u_\beta)^T$, the output matrix coefficient is $B = \begin{pmatrix} \frac{1}{L_S} & 0 & 0 & 0 \\ 0 & 0 & 0 & \frac{1}{L_S} \end{pmatrix}^T$, the output matrix is $C = \begin{pmatrix} 1 & 0 & 0 & 0 \\ 0 & 1 & 0 & 0 \end{pmatrix}$, and the output is $y = (i_\alpha, i_\beta)^T$.

5. Simulation analysis of motor control system based on EKF

5.1. Simulation experiment of motor operation after applying EKF algorithm

The simulation model of brushless DC motor control combined with the EKF algorithm is shown in **Figure 2**:

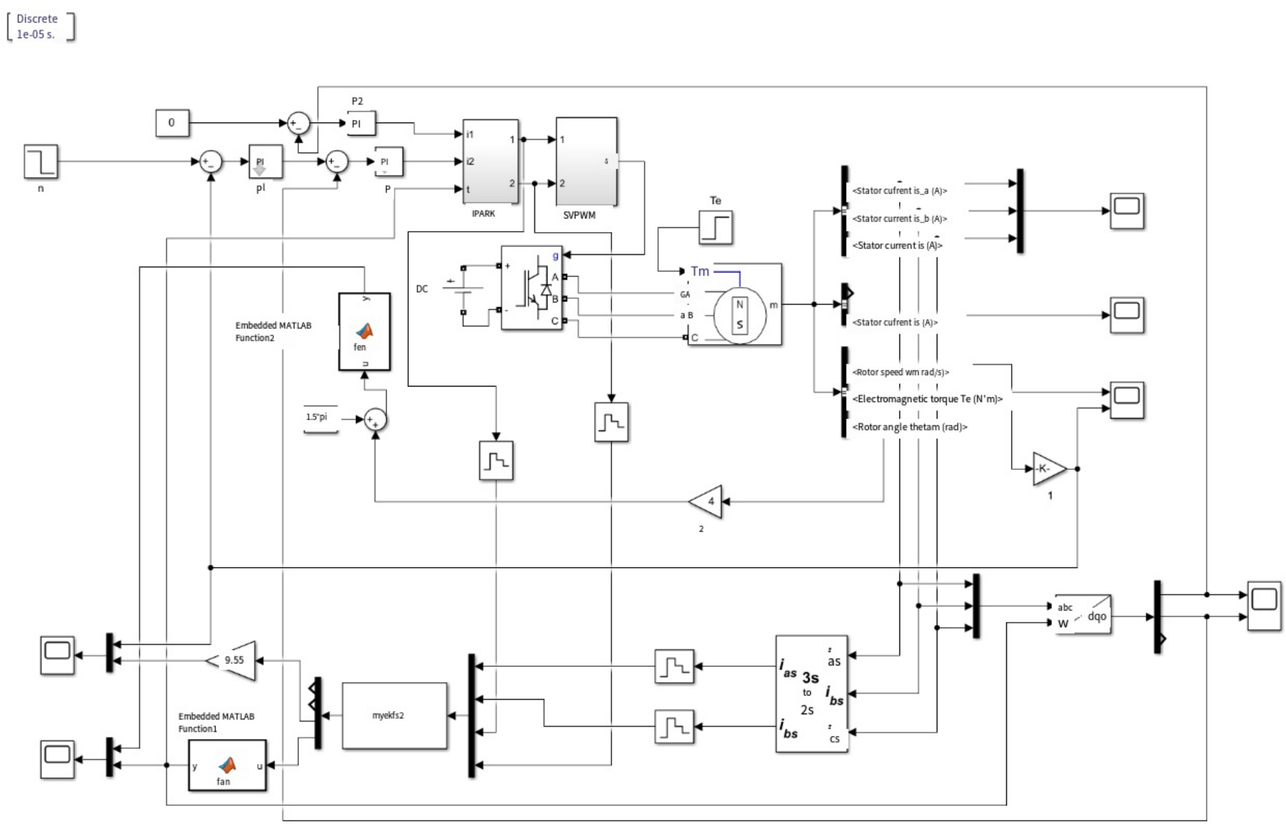

Figure 2. Simulink simulation model

The three-phase current waveforms after applying the EKF module are shown in **Figure 3**. It can be seen from the waveforms that the three-phase sine waves are 120° apart, and the current waveforms are relatively smooth and stable. The motor can operate normally under this simulation system.

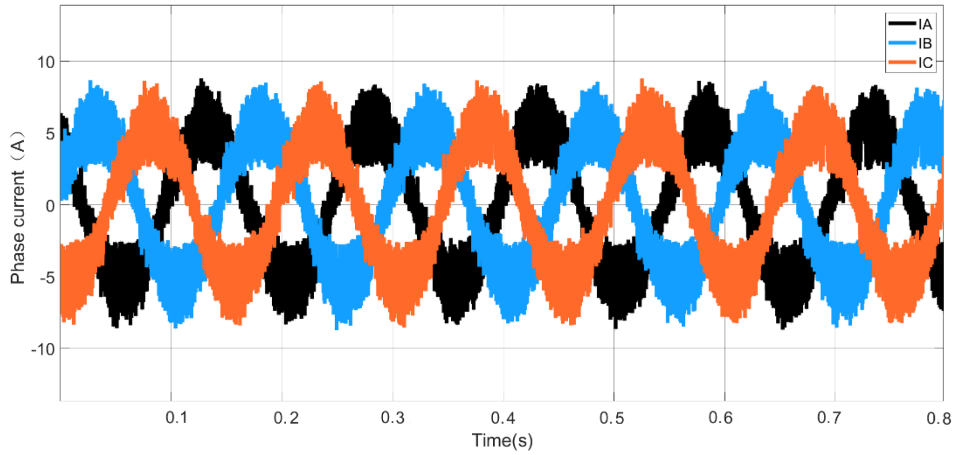

Figure 3. The three-phase current waveforms based on the EKF algorithm

5.2. Motor low-speed performance experiment based on EKF algorithm

The greatest advantage of EKF is to improve the low-speed performance of the motor. **Figures 4** and **5** show the rotational test curves of the motor with the encoder signal at 15rad/s. The system responds quickly and can be stable for short periods, but there is a certain error from the given speed, as can be seen from the rotation error curve in **Figure 5**, the maximum error is up to 0.7rad/s. When the system is in a stable state, its speed error remains at 6.7r/min.

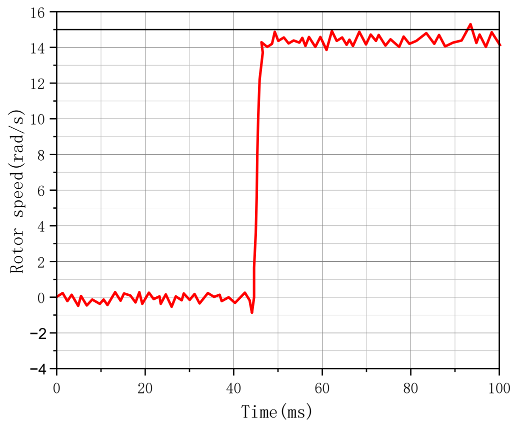

Figure 4. Rotation curve of 15rad/s motor

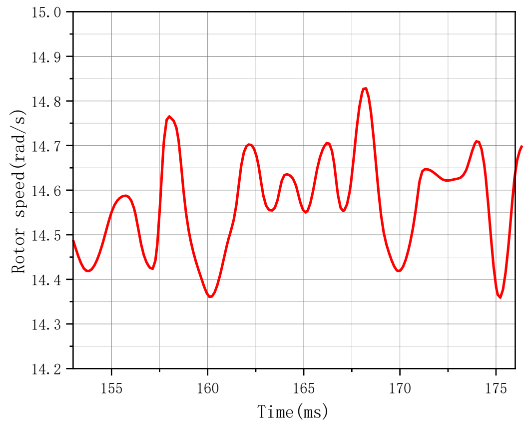

Figure 5. Rotation error curve of 15rad/s motor

Figures 6 and **7** show the test curves of the motor at a speed of 15rad/s with the addition of the EKF algorithm. It can be seen from the curves that the system responds very quickly, stabilizes at the set speed of 15rad/s very quickly, and the fluctuation range of the steady-state value is very small. It can be seen from **Figure 7** that the maximum error does not exceed 0.3rad/s. From the perspective of rotational speed, the speed error when the system is stable is 2.9r/min.

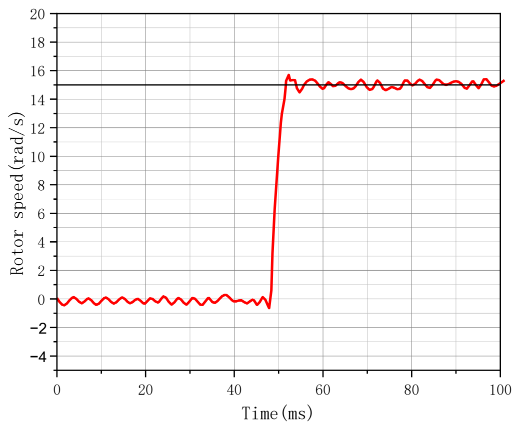

Figure 6. Rotation curve of 15rad/s motor

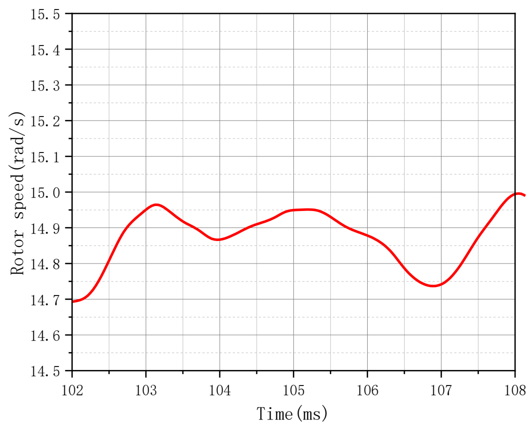

Figure 7. Rotation error curve of 15 rad

The Angle tracking curves estimated by the EKF algorithm and observed with normal motor rotation are shown in **Figure 8**, which is also the output of the EKF iteration and represents the position of the rotor.

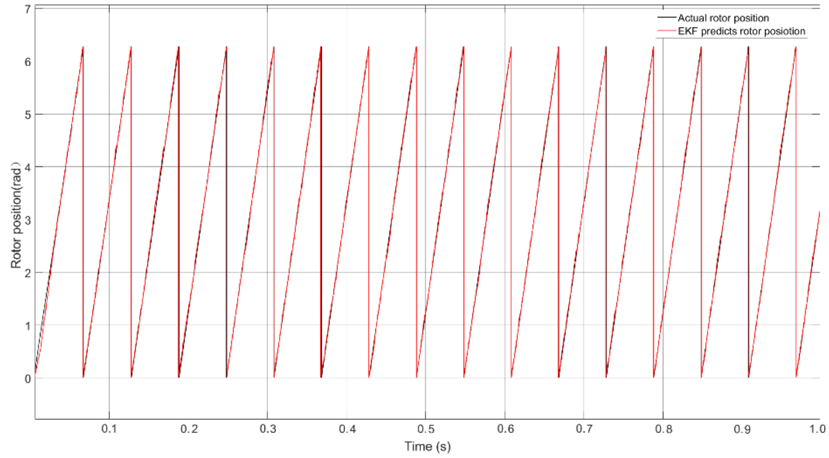

Figure 8. EKF rotor tracking

The black curve indicates the actual position of the rotor when the motor is running, and the red curve represents the rotor position estimated by the EKF algorithm. The motor starts running from rest. Before 0.2 seconds after starting, the estimated Angle by the EKF algorithm is slightly lower than the actual Angle of the motor rotor. After 0.2 seconds, the rotor Angle tracking is good. It can be seen that the EKF algorithm performs very well at low speeds, achieving very accurate estimates in an extremely short time [10].

It can be seen from **Figure 9** that at approximately 0.005s, the predicted speed of the EKF basically coincides with the actual speed curve, and the optimized EKF algorithm tracks very fast at low speed.

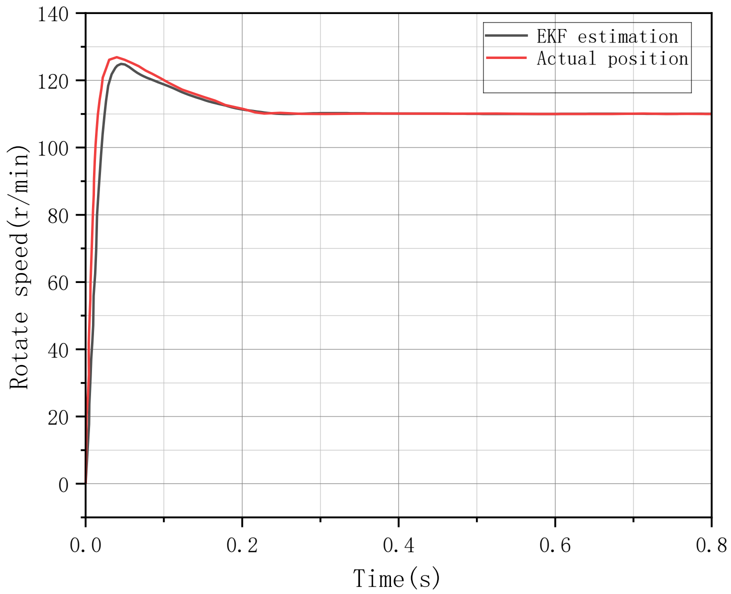

Figure 9. Speed tracking curve of the motor under no-load condition

It can be seen from **Figure 10** that when the load of the motor changes suddenly, the Angle of the rotor predicted by the EKF algorithm coincides with the actual Angle of the rotor, and the tracking effect is very good with a very small Angle error.

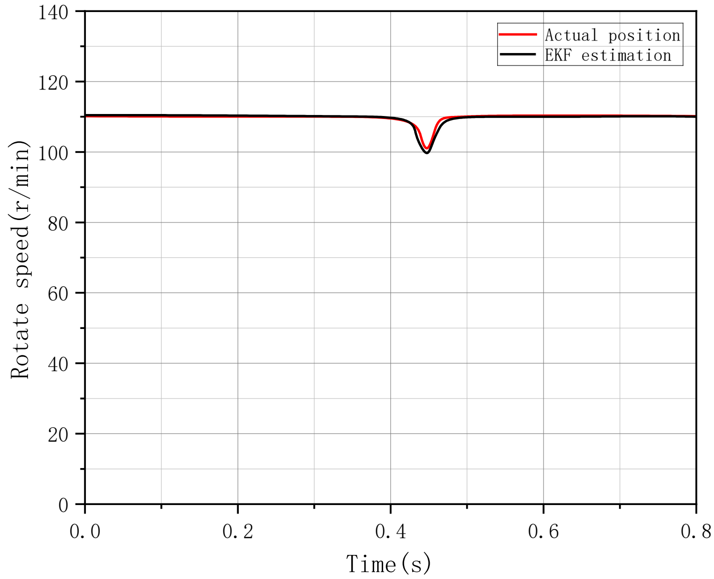

Figure 10. Speed tracking curve for sudden changes in motor load

From the above experiments, it can be seen that the EKF algorithm demonstrates outstanding control performance in the brushless DC motor position vectorless control system, especially in the low-speed operation state of the motor, showing good low-speed control performance and anti-interference ability, and the rotor position tracking effect is also very ideal, fully meeting the requirements of the system for the parameter control of the brushless DC motor [11].

6. Conclusions

This paper applies the EKF algorithm to the brushless DC motor control system by building a MATLAB simulation model of the BLDC position-free vector control system based on the EKF algorithm. The simulation results show that the non-position EKF algorithm performs well in the speed tracking and rotor position tracking experiments of the motor running at low speed. The tracking waveform is smooth and stable with high anti-interference ability, meeting the real-time requirements for motor control and achieving stable operation of the motor, providing a certain reference for the control strategy of brushless DC motors [12].

Disclosure statement

The authors declare no conflict of interest.

References

[1] Yu B, 2021, Research on Sensorless Control Technology for Brushless DC Motors at Full Speed Range, dissertation, Harbin Institute of Technology.

[2] Inan R, 2024, An Improved Model Predictive Current Control of BLDC Motor with a Novel Adaptive Extended

Kalman Filter–Based Back EMF Estimator and a New Commutation Duration Approach for Electrical Vehicle. International Journal of Circuit Theory and Applications, 53(2): 1135–1150.

[3] Li D, 2021, Low-speed Performance Improvement of Induction Motor Without Speed Sensor based on EKF Vector Control, dissertation, Xi'an University of Technology.

[4] Zheng X, 2021, Research on Sensorless Control Algorithm for BLDC based on Improved Kalman Filtering, dissertation, Harbin Institute of Technology.

[5] Hooshmand M, Yaghobi H, Jazaeri M, 2023, Speed and Rotor Position Estimation for Sensorless Brushless DC Motor Drive based on Particle Filter. Electrical Engineering, 105(3): 1797–1810.

[6] Matyuschenko A, 2015, Mathematical Field Models of Brushless DC Motors with Permanent Magnets and Their Comparative Analysis. Electrical Engineering & Electromechanics, (1): 25–28.

[7] Yingjun S, Zhenglong W, Yuanyuan F, 2025, An Adaptive Extended Kalman Filter Observer for Permanent Magnet Synchronous Motor Position Sensorless Control Systems. Scientific Reports, 15(1): 11605.

[8] Meysam H, Hamid Y, Mostafa J, 2023, Speed and Rotor Position Estimation for Sensorless Brushless DC Motor Drive based on Particle Filter. Electrical Engineering, 105(3): 1797–1810.

[9] Shao J, 2025, Dual-vector model predictive current control for brushless DC motors. Journal of Physics: Conference Series, 2963(1): 012020.

[10] Wang J, 2023, Research on Key technologies for Drive Control of Integrated Brushless DC motors, dissertation, University of Electronic Science and Technology of Xi'an.

[11] Shin Y, Kim K, Cho Y, et al., 2025, Rotor Position Estimation Error Compensation Using Back-EMF Based Sensorless Control for Low-Speed Operation in Washing Machines. Journal of Electrical Engineering & Technology, 20(4): 2497–2507.

[12] Yan X, 2020, Design and Implementation of FOC Control System for Sensorless BLDCM, dissertation, University of Electronic Science and Technology of China.